ELSEVIER

NeuroImage

www.elsevier.com/locate/ynimg
NeuroImage 35 (2007) 488–500

Regional coherence changes in the early stages of Alzheimer's disease: A combined structural and resting-state functional MRI study

Yong He,[a] Liang Wang,[b,c] Yufeng Zang,[a,d] Lixia Tian,[a] Xinqing Zhang,[e] Kuncheng Li,[b,c,*] and Tianzi Jiang[a,*]

[a]*National Laboratory of Pattern Recognition, Institute of Automation, Chinese Academy of Sciences, Beijing 100080, PR China*
[b]*Department of Radiology, Xuanwu Hospital of Capital Medical University, Beijing 100053, PR China*
[c]*Key Laboratory for Neurodegenerative Diseases (Capital Medical University), Ministry of Education, PR China*
[d]*State Key Laboratory of Cognitive Neuroscience and Learning, Beijing Normal University, Beijing 100875, PR China*
[e]*Department of Neurology, Xuanwu Hospital of Capital Medical University, Beijing 100053, PR China*

Received 9 January 2006; revised 14 November 2006; accepted 14 November 2006
Available online 24 January 2007

Recent functional imaging studies have indicated that the pathophysiology of Alzheimer's disease (AD) can be associated with the changes in spontaneous low-frequency (<0.08 Hz) blood oxygenation level-dependent fluctuations (LFBF) measured during a resting state. The purpose of this study was to examine regional LFBF coherence patterns in early AD and the impact of regional brain atrophy on the functional results. Both structural MRI and resting-state functional MRI scans were collected from 14 AD subjects and 14 age-matched normal controls. We found significant regional coherence decreases in the posterior cingulate cortex/precuneus (PCC/PCu) in the AD patients when compared with the normal controls. Moreover, the decrease in the PCC/PCu coherence was correlated with the disease progression measured by the Mini-Mental State Exam scores. The changes in LFBF in the PCC/PCu may be related to the resting hypometabolism in this region commonly detected in previous positron emission tomography studies of early AD. When the regional PCC/PCu atrophy was controlled, these results still remained significant but with a decrease in the statistical power, suggesting that the LFBF results are at least partly explained by the regional atrophy. In addition, we also found increased LFBF coherence in the bilateral cuneus, right lingual gyrus and left fusiform gyrus in the AD patients. These regions are consistent with previous findings of AD-related increased activation during cognitive tasks explained in terms of a compensatory-recruitment hypothesis. Finally, our study indicated that regional brain atrophy could be an important consideration in functional imaging studies of neurodegenerative diseases.

Keywords: Alzheimer's disease; Default mode; Functional connectivity; Morphometry; Neuroimaging; Posterior cingulate cortex; Resting state; Spectrum

Introduction

Functional neuroimaging studies of Alzheimer's disease (AD) typically focus on exploring activation (Buckner et al., 2000; Grady et al., 1993; Remy et al., 2005) or deactivation (Rombouts et al., 2005; Lustig et al., 2003) alterations in patients during a task state compared with a baseline state. Many neuroimaging studies also use the resting state to examine AD-related changes in brain activity. For instance, positron emission tomography (PET) and single-photon emission computerized tomography (SPECT) studies have found that AD patients have abnormally low resting cerebral blood flow (CBF) or cerebral metabolic rate for glucose (CMRGlu) in the posterior cingulate, parietal, temporal, and prefrontal cortex (Bokde et al., 2001; Herholz et al., 2002; Ibáñez et al., 1998; Leon et al., 2001; Salmon et al., 2000).

Recently, functional MRI (fMRI) studies have indicated that the pathophysiology of AD can be associated with the changes in spontaneous low-frequency (<0.08 Hz) blood oxygenation level-dependent (BOLD) fluctuations (LFBF) measured during a resting state. As early as 1995, Biswal et al. (1995) found that spontaneous LFBF measured by resting-state fMRI was highly synchronous within the somatomotor system and concluded that it was

* Corresponding authors. T. Jiang is to be contacted at National Laboratory of Pattern Recognition, Institute of Automation, the Chinese Academy of Sciences, Beijing 100080, PR China. Fax: +86 106255 1993. K. Li, Department of Radiology, Xuanwu Hospital of Capital Medical University, Beijing 100053, PR China.
E-mail addresses: jiangtz@nlpr.ia.ac.cn (T. Jiang), li_cums@yahoo.com.cn (K. Li).
Available online on ScienceDirect (www.sciencedirect.com).

1053-8119/$ - see front matter © 2006 Elsevier Inc. All rights reserved.
doi:10.1016/j.neuroimage.2006.11.042

physiologically meaningful. Following that study, high LFBF synchrony in healthy adults was also reported within the primary motor (Lowe et al., 1998; Cordes et al., 2001; Jiang et al., 2004), auditory (Cordes et al., 2001), and visual cortices (Kiviniemi et al., 2004, 2005; Lowe et al., 1998), as well as the nonprimary regions such as hippocampus (Rombouts et al., 2003), language (Hampson et al., 2002) and limbic systems (Greicius et al., 2003; Fox et al., 2005). Several recent studies have suggested that the LFBF can also be employed to characterize the pathophysiological changes of brain disorders, such as multiple sclerosis (Lowe et al., 2002), depression (Anand et al., 2005), schizophrenia (Liu et al., 2006), attention deficit hyperactivity disorder (ADHD) (Zang et al., in press; Cao et al., 2006) and acute brainstem ischemia (Salvador et al., 2005). To our knowledge, only three prior studies have examined AD-related LFBF activity using resting-state fMRI (Li et al., 2002; Maxim et al., 2005; Wang et al., 2006). In the first report, Li et al. (2002) exclusively examined functional synchrony of LFBF in the hippocampus and found it decreased significantly in the AD patients. The second study from Maxim et al. (2005) found that AD patients had greater persistence of resting fMRI noise in the medial and lateral temporal lobes, dorsal cingulate/medial premotor cortex, and insula. A very recent study from our research group found that AD patients showed abnormal hippocampal connectivity during resting state (Wang et al., 2006). Aside from these pure resting-state fMRI studies, using a low-frequency component derived from a simple sensory-motor task, Greicius et al. (2004) found that AD patients exhibited decreased resting-state activity within a default-mode network including the posterior cingulate cortex and inferior parietal lobe. Despite the limited number of reports, such intriguing studies have provided an insight into the pathophysiology of AD by means of spontaneous LFBF measured during rest. Of these, however, only one examined AD-related regional LFBF activity across the entire cortex (Maxim et al., 2005).

The first purpose of this study was to clarify and expand on AD-related regional LFBF changes by examining regional coherence in a pure resting state. Regional coherence was assessed using our previously published regional homogeneity (ReHo) method (Zang et al., 2004). In this study, we postulated that the medial parietal cortex [posterior cingulate cortex (PCC) and precuneus (PCu)] have decreased regional LFBF activity in the early stages of AD because the region is the most common site for AD-related functional changes such as the resting hypometabolism and hypoperfusion (Leon et al., 2001; Salmon et al., 2000; Volkow et al., 2002) and abnormal functional deactivation during the performance of cognitive tasks (Rombouts et al., 2005; Lustig et al., 2003). In addition, we also expected to observe AD-related LFBF changes in the other regions.

However, a number of key issues still remain given that we observed altered LFBF activity in the PCC/PCu and the other regions. The major concern is the possible impact of regional brain atrophy on the functional results. Many studies have indicated that AD patients have more brain tissue atrophy than normal controls in the PCC/PCu, medial temporal cortex, caudate nucleus and medial thalami (Rombouts et al., 2000; Karas et al., 2003; Baron et al., 2001). The brain atrophy may lead to artificial reduction in measured functional signals. While comparing functional differences between AD patients and normal controls, this issue could potentially be crucial due to individual and group differences in the degree of regional atrophy. Several PET studies have suggested that temporoparietal hypometabolism became nonsignificant in the AD patients after accounting for brain atrophy (Chawluk et al., 1990; Tanna et al., 1991). In fMRI studies, a few groups have made an attempt to explore the relationship between regional brain atrophy and functional activation in AD patients during cognitive tasks (Johnson et al., 2000; Prvulovic et al., 2002; Remy et al., 2005). To date, however, no studies have specifically examined the effect of brain atrophy on spontaneous LFBF measurements. Hence, determining the impact of regional atrophy on the LFBF results is the other purpose of this study.

To address these questions, in this resting-state study, we first used the ReHo method (Zang et al., 2004) to explore the changes of AD-related regional LFBF activity in the whole brain. The behavioral correlates of the LFBF activity were further examined in the AD patient group. Finally, the atrophy of the regions showing significant between-group ReHo difference was measured for each subject and its impact on the LFBF results was statistically evaluated.

Materials and methods

Subjects

Thirty subjects participated in this study. The 15 AD patients were recruited from Xuanwu Hospital, Capital Medical University. The 15 healthy elderly controls were recruited by advertisements from the local community. The elderly controls group and the AD group were matched by age (within 2 years) and gender. The older adults were assessed clinically with the Clinical Dementia Rating (CDR) score (Morris, 1993) as nondemented (CDR = 0) and the early stages of AD (7 participants with CDR = 0.5 and 8 participants with CDR = 1). The diagnosis criteria for AD fulfilled the Diagnostic and Statistic Manual Disorders, Fourth Edition (DSM-IV; American Psychiatric Association, 1994) criteria for dementia, and the National Institute of Neurological and Communicative Disorders and Stroke/Alzheimer Disease and Related Disorders Association (NINCDS-ADRDA) (McKhann et al., 1984) criteria for AD. All AD patients underwent a complete physical and neurological examination, an extensive battery of neuropsychological assessment and standard laboratory tests. The brain MRI scan for the AD patients showed no abnormality other than brain atrophy. All healthy controls had no history of any neurological or psychiatric disorders, sensorimotor impairment or cognitive complaints, and there were no abnormal findings observed in conventional brain MRI. Informed consent was obtained from all subjects and this study was approved by the human research ethics committee of Xuanwu Hospital of Capital Medical University. Data from two subjects were excluded due to excessive motion (see Data Preprocessing). Clinical and demographic data for the remaining 28 participants are shown in Table 1.

Table 1
Characteristics of the AD patients and normal controls

Characteristics	AD (n=14)	Controls (n=14)	P value
Sex, female/male	8/6	8/6	>0.99 †
Age, years	70.1±6.4	69.6±5.5	0.83 *
Handedness, right/left	14/0	14/0	>0.99 †
Education, years	9.4±4.9	9.4±4.2	0.97 *
MMSE	23.2±2.8	28.8±0.9	<0.0001 *

MMSE, Mini-Mental State Examination; Plus-minus values are means±S.D.
* The P value was obtained by a two-sample two-tailed t test.
† The P value was obtained by Pearson χ^2 two-tailed test, with continuity correction for $n<5$.

Data of 13 AD patients and 13 elderly controls had been used to study hippocampal functional connectivity changes in the AD patients (Wang et al., 2006).

Data acquisitions

All subjects were scanned on a Siemens 1.5 T Magnetom Sonata scanner (Siemens, Erlangen, Germany) equipped with a circularly polarized standard head coil. Foam pads and headphones were used to reduce head motion and scanner noise. Functional images were collected axially by using an echo-planar imaging (EPI) sequence [repetition time (TR)/echo time (TE)/flip angle (FA)/field of view (FOV)=2000 ms/60 ms/90°/24 cm, resolution=64×64 matrix, slices=20, thickness=5 mm, gap=2 mm, bandwidth=2442 Hz/pixel]. Subjects were instructed to keep their eyes closed, relax their minds and remain motionless as much as possible during the EPI data acquisition. The scan lasted for 360 s. At the same slice locations as the functional images, T1 anatomical images were acquired (TR/TE/FA/FOV=500 ms/7.7 ms/90°/24 cm, resolution=256×256 matrix, slices=20, thickness=5 mm, gap=2 mm). These images were used to coregister the functional images onto the anatomical 3D T1-weighted magnetization-prepared rapid gradient echo (MPRAGE) sagittal images [TR/TE/inversion time (TI)/FA=1970 ms/3.9 ms/1100 ms/15°, resolution=256×205 matrix, slices=96, thickness=1.7 mm].

Data preprocessing

Unless otherwise stated, all preprocessing were carried out using the AFNI package (Cox, 1996). The first 10 image acquisitions of the resting state were excluded from analysis because of the instability of the initial MRI signal and the adaptation of the subjects to the circumstances. The remaining 170 images acquisitions were first time-shifted using the sinc interpolation and then motion-corrected using a 3D volume registration program (Cox, 1996; Cox and Jesmanowicz, 1999). Two subjects' (one healthy elder adult and one AD subject with CDR=1) data were excluded from further analysis because of excessive movement (>1.5 mm or 1.5°). Moreover, we also performed a two-sample *t* test on the mean absolute estimated movement parameters (translation and rotation, respectively) on all three axes to examine between-group differences in the degree of head motion. Following the motion correction, all data were spatially normalized into Talairach and Tournoux coordinate space (Talairach and Tournoux, 1998) using a landmark-based 12 sub-volume piecewise linear method (Cox, 1996). After this, the functional images were then re-sampled to 3-mm isotropic voxels followed by spatial smoothing with a 4-mm full width at half maximum (FWHM) Gaussian kernel. Finally, temporal filtering (0.01 Hz<f<0.08 Hz) was performed on the time series of each voxel to reduce the effect of low-frequency drifts and high-frequency noise (Biswal et al., 1995; Lowe et al., 1998; Jiang et al., 2004). One of the healthy elder subjects did not have 20-slice anatomical data, the spm2 (www.fil.ion.ucl.ac.uk/spm) was used to coregister this subject's functional images to her own 3D anatomical images that were later transformed into Talairach and Tournoux coordinates space (Talairach and Tournoux, 1998). A mask file was created according to the intersection of the normalized T1 anatomical images (Wang et al., 2006). Only the voxels within the mask were further analyzed. The mask file was also used for correcting multiple comparisons later.

Data analysis

Functional and anatomical data were analyzed using MATLAB (The MathWorks, Inc., Natick, MA) programs, unless mentioned otherwise.

ReHo analyses

A within-subject analysis was first performed using the ReHo approach (Zang et al., 2004). The ReHo method, unlike the connectivity-based methods typically used in most LFBF studies, is suitable for exploring regional brain activity during rest by examining the degree of regional coherence of fMRI time courses. This is accomplished on a voxel-by-voxel basis by calculating Kendall's coefficient of concordance (KCC) (Kendall and Gibbons, 1990) of time series of a given voxel with those of its nearest neighbors (see Appendix 1 for details). A larger value for a given voxel indicates a higher regional coherence within a cluster made up of the voxel and its nearest neighbors. An individual ReHo map during rest was thus obtained for each subject. To give a visual impression of ReHo, mean ReHo maps were obtained within each group (Fig. 1). In our methodology paper, we assumed that ReHo could be modulated in the pertinent experimental tasks and this was confirmed by examining the modulation from a motor task to a resting state (Zang et al., 2004). In the present study, we extend our hypothesis as follows: ReHo is also different between AD patients and normal controls and it varies with the disease progression in patients. To explore the ReHo differences between the AD patient group and the control group, a random-effects two-sample *t* test (Holmes and Friston, 1998) was carried out on individual ReHo map in a voxel-wise way by taking age as a confounding covariate. In this study, the ages did not show significant differences between groups (P=0.83). However, to ensure that any significant differences were not the result of an undetected age effect, age was still included as a covariate in the functional analyses.

To control Type I error in this analysis, Monte Carlo simulations were performed using the AFNI AlphaSim program (parameters were: individual voxel P value=0.02, 10,000 simulations, FWHM=4 mm, with mask). By iterating the process of random image generation, spatial correlation of voxels, thresholding and cluster identification, the program provides an estimate of the overall significance level achieved for various combinations of individual voxel probability threshold and cluster size threshold (Poline et al., 1997). Using this program, a corrected significance level of P<0.05 was obtained by clusters with a minimum volume of 513 mm^3 at an uncorrected individual voxel height threshold of P<0.02. This enabled the identification of significant changes in ReHo in the AD patients as compared with the normal controls. It was noted that, in this study, we performed Monte Carlo simulations in the Talairach space (Talairach and Tournoux, 1998) at the interpolated resolution of 3 mm×3 mm×3 mm. We applied a 4 mm FWHM, the spatial smoothing kernel used in data preprocessing, for the Alphasim procedure due to the fact that there are no definite approaches to estimate an accurate effective FWHM, though it could overestimate the cluster significance observed in this study.

Correlations between ReHo and MMSE in the AD group

In order to explore whether the ReHo measurements vary with the disease progression in the AD patients, multiple regression analysis of ReHo versus Mini-Mental State Examination (MMSE) score was performed as follows. First, ReHo of the peak voxel in

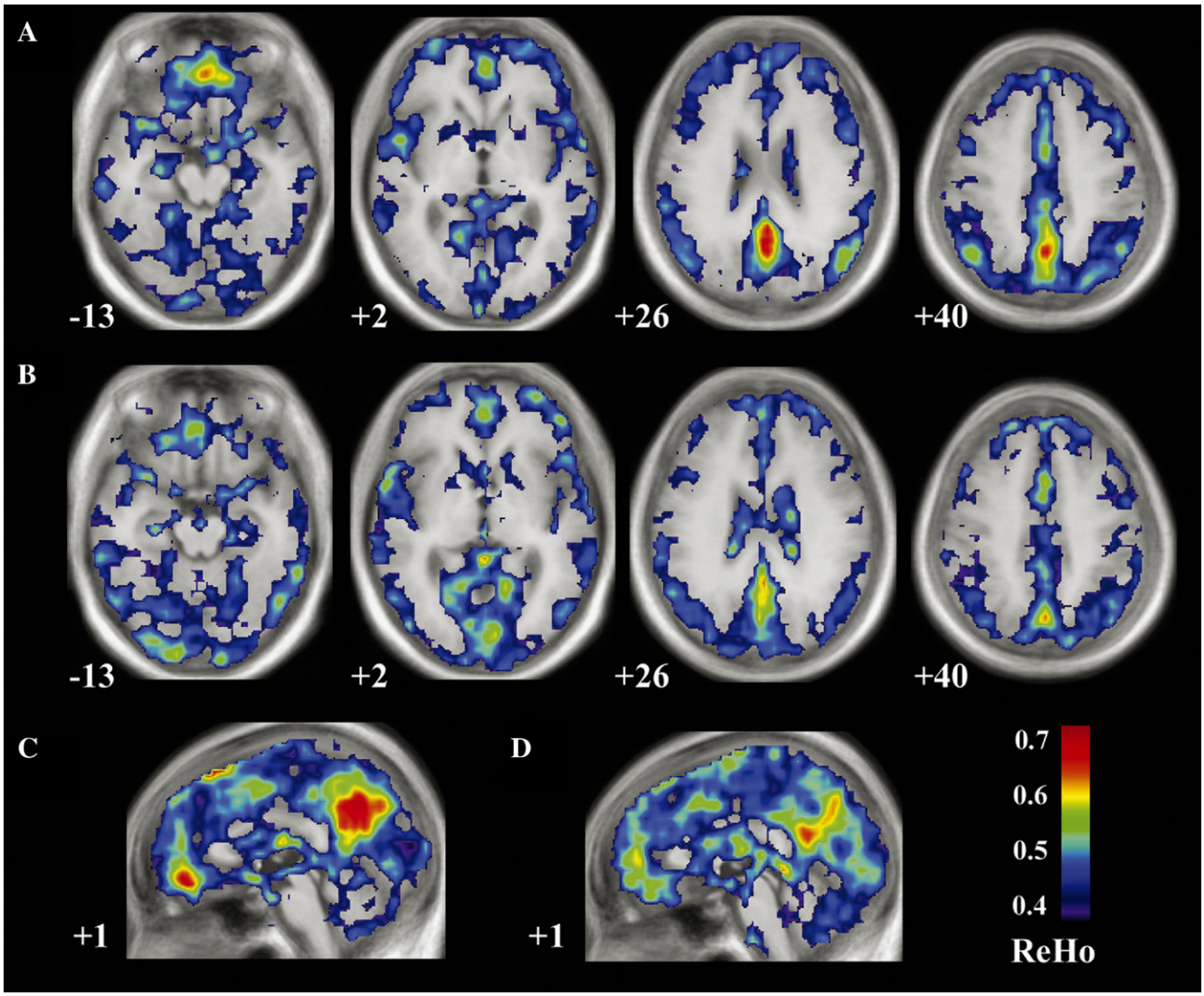

Fig. 1. Mean ReHo maps within the normal controls group (A) and AD patients group (B). Visual examination indicates high ReHo values in several default-mode regions, including the PCC/PCu, medial prefrontal cortex, dorsal lateral prefrontal cortex and inferior parietal cortex within each group, but a different strength between the groups. To visually highlight the ReHo difference in the PCC/PCu between the two groups, we also showed a sagittal view of this region for the normal controls group (C) and AD patients group (D). The functional results were overlaid on the transverse sections of the group-average structural images. For panels A and B, the numbers below each image refer to the *z* plane coordinates of Talairach and Tournoux. Left side of the image corresponds to the right side of the brain. For panel C and D, the numbers below each image refer to the *x* plane coordinates of Talairach and Tournoux. Left side of the image corresponds to the anterior part of the brain. Color bar is shown on the right.

each region showing significant between-group difference was correlated with the MMSE score in the AD patient group. Secondly, to ascertain whether these correlations are regional-specific or global effects, the regression model of ReHo versus the MMSE score was also performed in the AD patients at each voxel of the whole brain. The statistical map was corrected for multiple comparisons to a significant level of $P<0.05$ by combining the individual voxel P value <0.02 with cluster size >513 mm^3 using Monte Carlo simulations as described in previous section. Individual ages were entered as a covariate in these regression analyses.

Measurements of regional brain atrophy

In order to investigate the impact of regional brain atrophy on the functional results above, we calculated a regional atrophy index of each region showing significant between-group ReHo difference as follows. First, the Talairach-normalized and re-sampled (1 mm^3) 3D anatomical images of each subject within the brain mask were automatically segmented into gray matter, white matter and cerebrospinal fluid (CSF) by using a multicontext fuzzy clustering method (Zhu and Jiang, 2003). This segmentation method reduces the effects of both artificial and inherent intensity inhomogeneities. In the next step the regions exhibiting significant between-group ReHo differences were defined as group regions of interest (ROIs). The regional atrophy index of each region was calculated by dividing the volume of brain tissue by the total volume of the corresponding ROI (brain tissue+CSF). The value of individual regional atrophy index is ranged from 0 to 1. A higher value indicates a smaller amount of atrophy in this region. The atrophy

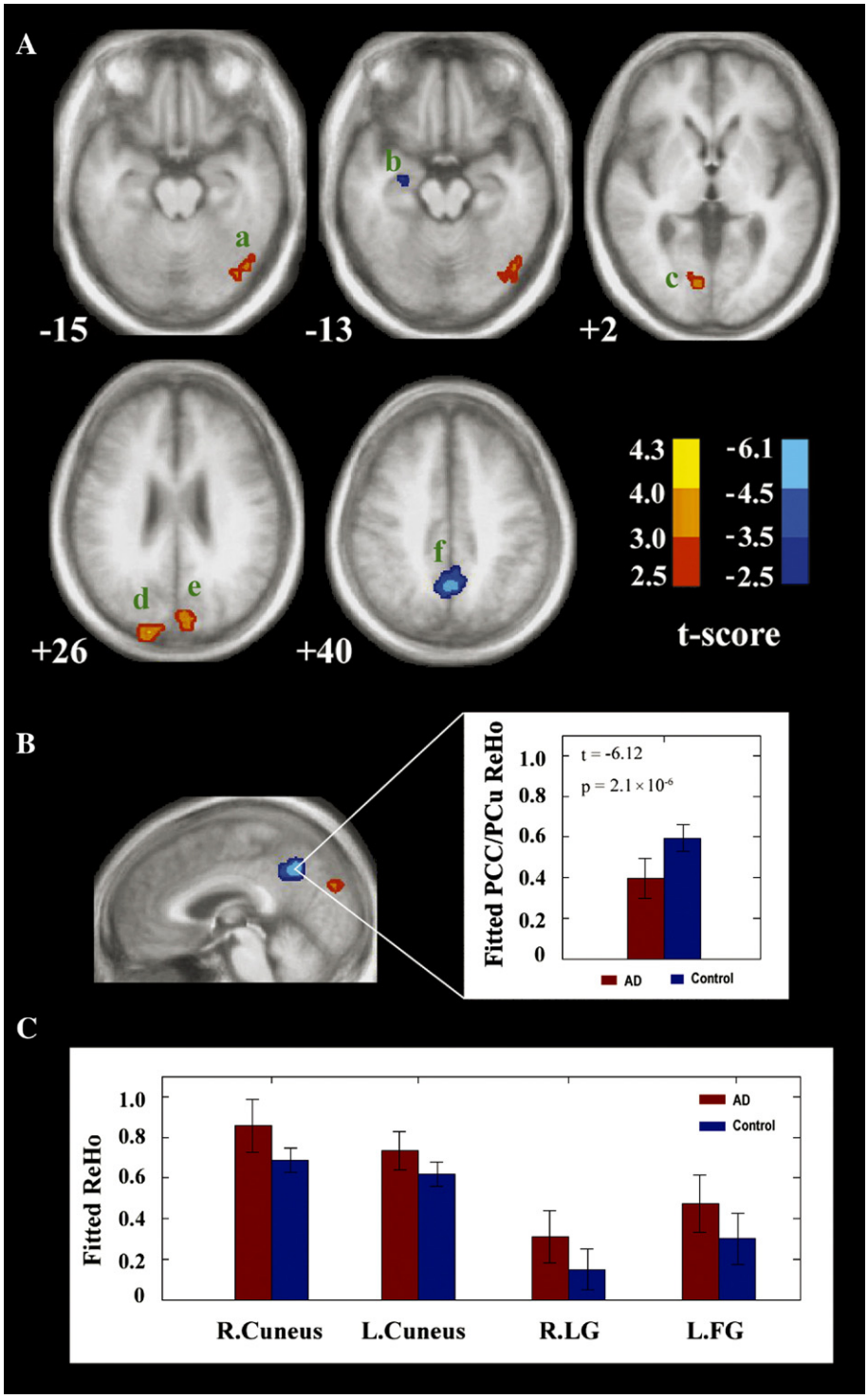

Fig. 2. (A) *t*-statistical difference map between the AD patients and normal controls (age effect removed by regression). The AD patients showed significant increased ReHo in the left FG (a), right LG (c), right cuneus (d) and left cuneus (e) and decreased ReHo in the PCC/PCu (f). The images also showed a 243-mm^3 cluster in the right hippocampus (b) that survived the height but not the extent threshold (AD patients < normal controls). *T*-score bars are shown on the right. Hot and cold colors indicate AD-related ReHo increases and decreases, respectively. Voxels with $P<0.02$ and cluster size of 513 mm^3 were used to identify significant clusters. These criteria met a corrected threshold of $P<0.05$. For other details, see Fig. 1. (B) A sagittal view of the *t*-statistical map highlights the between-group ReHo difference in the PCC/PCu. Bar graphs indicate that mean fitted ReHo of peak voxel with standard error (arbitrary units) bars of the PCC/PCu in AD patients versus normal controls (age effect removed by regression). The patients showed significant decreased ReHo in the PCC/PCu ($P=2.1\times10^{-6}$). (C) Mean fitted ReHo of peak voxel with standard error (arbitrary units) bars of the bilateral cuneus, right LG and left FG in AD patients versus normal controls (age effect removed by regression). Bar graphs indicate that the patients showed significantly increased ReHo in the right cuneus ($P=0.0002$), left cuneus ($P=0.0008$), right LG ($P=0.0013$) and left FG ($P=0.0026$). Further details of these regions are presented in Table 2.

index measurements in this study are similar to those proposed by two previous studies (Johnson et al., 2000; Prvulovic et al., 2002). Finally, a two-tailed two-sample t test was performed on the index of each region to compare the difference of regional atrophy between the AD patient group and the control group.

Effect of regional atrophy on LFBF analysis

To determine to what extent the functional results were influenced by the brain atrophy, we further examined the between-group differences in peak voxel ReHo using a two-sample t test by taking individual regional atrophy indices and ages as covariates. Additionally, the correlation of peak voxel ReHo and the MMSE score in the AD group was also examined by a regression analysis. This analysis included individual regional atrophy indices and ages as covariates. Finally, the statistical significances were compared with the functional results obtained from the same processes but without accounting for the regional atrophy.

Results

Characteristics of the AD patients and the normal controls are shown in Table 1. There were no significant differences between the AD patients and normal controls in gender, age, handedness and years of education, but the MMSE scores were significantly different ($P<0.0001$) between the two groups. Examination of movement parameters demonstrated that there were no significant differences (translation: $t=1.6$, $P=0.19$; rotation: $t=1.22$, $P=0.23$) in the degree of head motion between the AD patient group and the control group.

Within-group and between-group ReHo analyses

The mean ReHo maps within each group are shown in Fig. 1. Visual inspection indicates that the PCC/PCu has the highest ReHo value within each group but different strength between the groups (Fig. 1). In addition, we also find that other brain regions, including medial prefrontal cortex, dorsal lateral prefrontal cortex and inferior parietal cortex, have high ReHo values within each group. The ReHo pattern is very similar to a default-mode network proposed by Raichle et al. (2001) from a PET study. Here these within-group maps are merely for visualizing ReHo. The results obtained from the two-sample t test clearly showed significant ReHo differences between the two groups (Fig. 2, Table 2). Compared with the healthy controls, the AD patients showed significant ReHo decreases in the PCC/PCu [Brodmann's area (BA) 31/7] and increases in the occipital and temporal lobes, including the bilateral cuneus (BA 19), right lingual gyrus (LG, BA 18) and left fusiform gyrus (FG, BA 37). Additionally, we also found a 243-mm^3 cluster in the right hippocampus that survived the height but not the extent threshold (AD patients < normal controls, Fig. 2).

Table 2
Regions showing regional coherence changes in the AD patients

Brain regions	BA	Vol, mm^3	Stereotaxic coordinates, mm			Maximum t
			x	y	z	
PCC/PCu	31/7	2430	1	−57	40	−6.12
Right hippocampus		243	24	−12	−11	−3.97[a]
Right cuneus	19	783	15	−88	26	4.32
Left cuneus	19	864	−7	−77	26	3.79
Right LG	18	999	5	−74	2	3.62
Left FG	37	567	−45	−65	−15	3.34

BA, Brodmann's area; Vol, cluster volume; x, y, z, coordinates of primary peak locations in the space of Talairach and Tournoux (1998); t, statistical value of peak voxel showing ReHo differences between groups (positive t value means decreased ReHo in the AD group); PCC/PCu, posterior cingulate cortex/precuneus; Hipp, hippocampus; LG, lingual gyrus; FG, fusiform gyrus.

[a] The region in the right hippocampus survived the height but not the extent threshold. $P<0.05$, corrected for multiple comparisons.

Correlations between ReHo and MMSE in the AD group

Regression analysis revealed a significant correlation between peak voxel ReHo in the PCC/PCu ($t=3.51$, $P=0.005$) and the MMSE scores in the AD group (Fig. 3). However, there were no significant correlations found in the right cuneus ($t=-0.54$, $P=0.60$), left cuneus ($t=0.39$, $P=0.71$), right LG ($t=1.21$, $P=0.25$) and left FG ($t=-1.08$, $P=0.30$). Further analysis by regressing ReHo at each voxel in the whole brain against the MMSE score in the AD patients group revealed that the most significant positive correlation occurs in the PCC/PCu (BA 31/7) (Fig. 3, Table 3). Moreover, significant positive correlations were also found in the right cerebellum, right inferior parietal lobe and right angular gyrus; significant negative correlations in the bilateral inferior frontal gyrus, medial prefrontal cortex, left cuneus and left precentral gyrus (Fig. 3, Table 3).

Examination of regional brain atrophy

The two-sample t test revealed that the AD patients had more brain tissue atrophy than normal controls in the PCC/PCu ($t=-2.08$, $P=0.047$) (Fig. 4A). There was no significant atrophy observed in the right cuneus ($t=0.44$, $P=0.67$), left cuneus ($t=-1.18$, $P=0.25$), right LG ($t=-1.69$, $P=0.11$) and left FG ($t=0.80$, $P=0.25$) in the patients (Fig. 4A).

Effect of regional atrophy on LFBF analysis

Of all the regions showing AD-related LFBF changes, only PCC/PCu demonstrated both significant ReHo decreases and brain tissue atrophy. In this study, we thus evaluated the impact of regional atrophy on the functional results shown in the PCC/PCu. After controlling for the regional atrophy by statistical analysis (the regional atrophy index and age were used as covariates), significant PCC/PCu ReHo differences ($t=-5.25$, $P=2.2\times10^{-5}$, Fig. 4B) between the two groups and significant correlation of PCC/PCu ReHo against the MMSE score ($t=2.50$, $P=0.031$, Fig. 4C) in the patients group was still observed. However the statistical significance was obviously reduced (Figs. 4B and C) compared to the results without accounting for the regional atrophy (Figs. 2B and 3B).

Discussion

Our study investigates AD-related LFBF changes and the impact of regional brain atrophy on the LFBF results. Compared with healthy controls, the AD patients showed decreased regional coherence (i.e. ReHo) in the PCC/PCu and increased coherence in

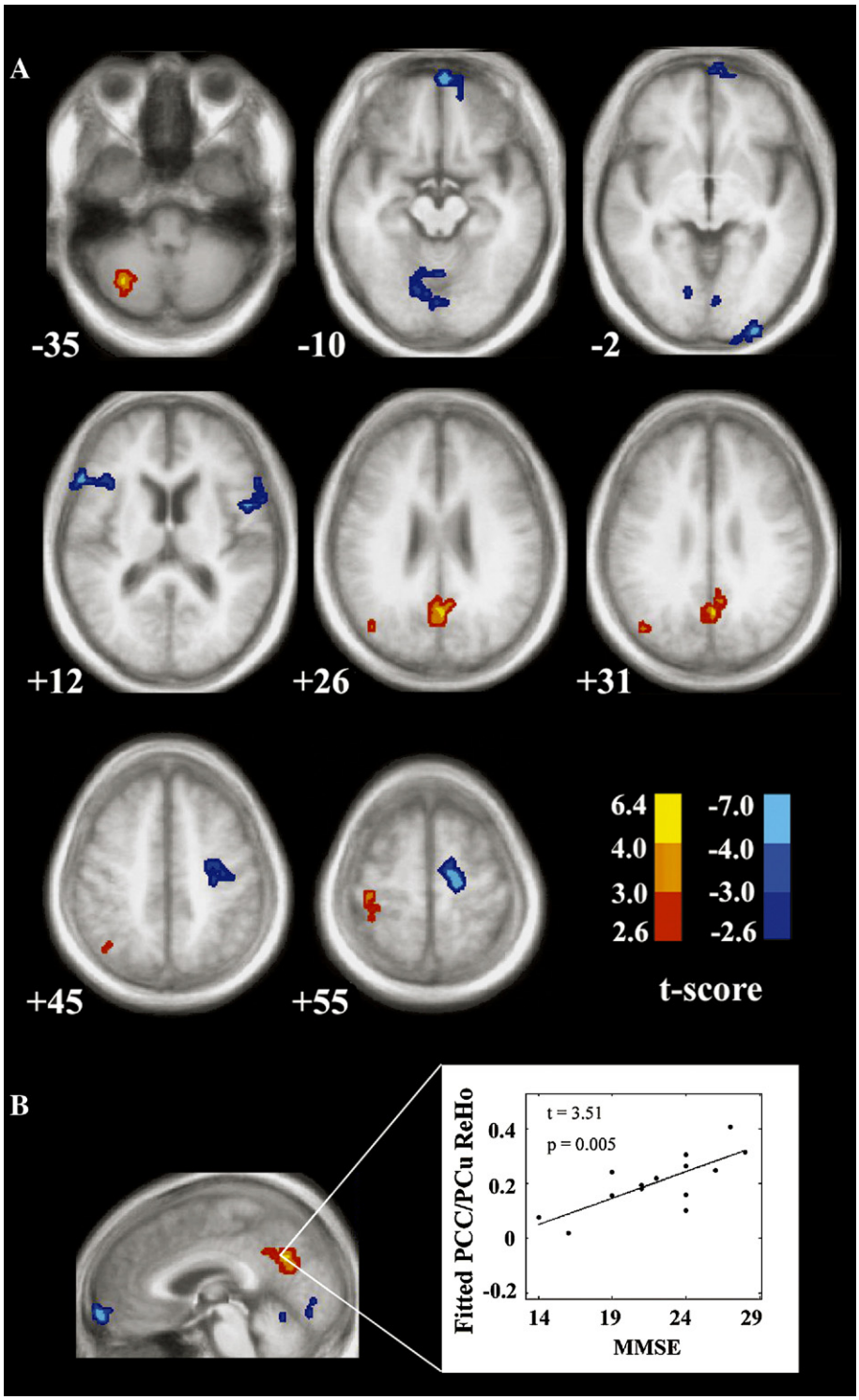

Fig. 3. (A) *t*-statistical map of the MMSE regression against ReHo in the AD patient group ($n=14$) (age effect removed by regression). (B) A sagittal view of the *t*-statistical map highlights significant positive correlation between the PCC/PCu ReHo and MMSE scores. Scatter plot of fitted ReHo of peak voxel in the PCC/PCu (i.e. the voxel showing the most significant ReHo decrease between the two groups) versus MMSE scores in the patient group was shown on the right side (age effect removed by regression). Each data point represents a single subject in the AD group. Aside from the PCC/PCu, many other regions also show significant associations between the ReHo and MMSE scores. Further details of these regions are presented in Table 3. Voxels with $P<0.02$ and cluster size of 513 mm^3 were used to identify significant clusters. These criteria met a corrected threshold of $P<0.05$. For other details, see Fig. 1.

Table 3
Regions showing significant correlations ($P<0.05$, corrected) in ReHo versus MMSE in the AD patient group

Brain regions	BA	Vol, mm^3	Stereotaxic coordinates, mm			Maximum t
			x	y	z	
PCC/PCu	31/7	1971	3	−56	31	6.46
Right cerebellum	N/A	999	27	−62	−35	4.89
Right AG	39	594	42	−67	31	4.65
Right IPL	40	756	36	−40	55	4.07
Left PrCG	4	1296	−15	−12	56	−7.09
MPFC	10	1161	0	63	−6	−6.58
Right cerebellum	N/A	1215	15	−65	−10	−5.37
Left IFG	44	1215	−48	10	14	−5.06
Right IFG	46	945	53	27	11	−4.91
Left cuneus	17	567	−18	−100	0	−4.62
Left PrCG	4	756	−28	−9	44	−4.24

BA, Brodmann's area; Vol, cluster volume; x, y, z, coordinates of primary peak locations in the space of "Talairach and Tournoux (1998); t, statistical value of peak voxel showing significant correlation of ReHo versus the MMSE score in the AD group (positive t value means positive correlation); PCC/PCu, posterior cingulate cortex/precuneus; AG, angular gyrus; IPL, inferior parietal lobe; PrCG, precentral gryus; MPFC, medial prefrontal cortex; IFG, inferior frontal gyrus; $P<0.05$, corrected for multiple comparisons.

the occipital and temporal lobe, including the bilateral cuneus, right LG and left FG. In addition, we also found that the PCC/PCu LFBF coherence reduces with the progress of the disease. Most importantly, these results still remain significant after statistically controlling for the regional atrophy. Taken together, our results are compatible with previous neuroimaging studies of early AD, which provides important insights into understanding the LFBF activity and its clinical implications.

It is important to look at coherent neuronal fluctuations and spontaneous low-frequency fluctuations observed in BOLD signal before our results are further interpreted. Although a large number of studies has shown coherent fluctuations in resting-state fMRI within different neuro-anatomical systems (Biswal et al., 1995; Fox et al., 2005; Greicius et al., 2003; Lowe et al., 1998; Rombouts et al., 2003; He et al., 2006; Salvador et al., 2005; Jiang et al., 2004), the origin of these coherences and the neurophysiological basis of the LFBF remain unclear to date. Nevertheless, some investigators have suggested that the LFBF might be associated with neuronal firing in the resting state (Biswal et al., 1997; Maldjian, 2001). In conventional task-specific fMRI studies, such LFBF is usually considered noise and excluded using filtering techniques. However, recent studies have suggested that coherent spontaneous activity is expressed in larger neuronal populations (Arieli et al., 1996; Leopold et al., 2003). Moreover, it has been shown that each region of the nervous system can generate its own cyclical patterns that interact with those of the other regions to which it is connected (Steriade et al., 1993). These spontaneous activities are physiologically meaningful for keeping a balance between regional and global processing in the default resting state. Recent studies have suggested that some specific brain diseases such as multiple sclerosis (Lowe et al., 2002), ADHD (Zang et al., in press; Cao et al., 2006), depression (Anand et al., 2005) and AD (Greicius et al., 2004; Maxim et al., 2005; Li et al., 2002; Wang et al., 2006) exhibit abnormal regional and/or global coherent LFBF patterns.

In the present study, as expected, we found significant LFBF coherence decreases in the PCC/PCu in the AD patients (Fig. 2, Table 2). It has been shown that, in healthy subjects, the PCC/PCu has the highest metabolic rates (Raichle et al., 2001) and is considered a central node in a default-mode network during rest (Greicius et al., 2003). Moreover, this region has been observed with the highest coherence in both young (He et al., 2004; Zang et al., 2004) and old adults (Fig. 1) during rest. We will now consider the possible mechanisms behind the AD-related decreases in this region. The possible explanation could be that their presence was associated with resting hypometabolism in AD. Many PET studies have consistently shown reduced resting metabolism in the PCC/PCu in subjects with AD (Buckner et al., 2005; Leon et al., 2001; Salmon et al., 2000; Volkow et al., 2002) or cognitively intact subjects with genetic susceptibility to AD (Reiman et al., 1996; Small et al., 2000). In this regard, it is particularly instructive that Volkow et al. (2002) revealed not only reduced resting metabolism, but also decreased regional metabolic homogeneity in the PCC/PCu. In addition, it is also noted that resting metabolism in the PCC/PCu measured using fluorodeoxyglucose PET was correlated with the disease progress evaluated by the MMSE scores (Buckner et al., 2005; Herholz et al., 2002; Salmon et al., 2000). Our examination of the behavioral correlates of ReHo also revealed significant ($P<0.031$) positive correlation between the PCC/PCu ReHo measurements and the MMSE scores in the AD patient group (Figs. 3B and 4C). The combination of these findings raises the possibility of a relationship between decreased ReHo and reduced resting metabolism in this region. Though the mechanism of decreased PCC/PCu ReHo needs to be further clarified, the present study provides an important implication on regional AD-related LFBF abnormality in the resting state. The fact that this location was consistently found to have AD-related abnormality in many other functional imaging studies make us believe that this is an important region for clinical research of AD. In this study, we also found that AD patients had decreasing ReHo in the right hippocampus (Fig. 2A). A large number of studies have demonstrated that the hippocampus is one of the earliest regions affected by the accumulation of AD lesions (see Nestor et al., 2004 for a review). Two recent studies of resting-state fMRI have also suggested that the hippocampus has abnormally spontaneous LFBF activity in AD patients (Maxim et al., 2005; Li et al., 2002), which provides further support for our finding of reduced ReHo in this region.

Recently, two resting-state fMRI studies from Greicius et al. (2004) and our research group (Wang et al., 2006) have suggested that the AD patients showed mild decreased trends in the functional connectivity between the PCC/PCu and hippocampus. Using our ReHo measurement, we observed the decreased regional resting activity in both regions; one interesting question would be whether the AD patients also demonstrated decreased PCC/PCu-hippocampus connectivity in the present investigation. To address this issue, we performed a functional connectivity analysis as follows. The time series of two peak voxels in the PCC/PCu and hippocampus showing the most significant between-group ReHo differences were first extracted from each subject. Then, we calculated the Pearson correlation coefficients between the two regions and further transformed them into z values using the Fisher's z-transform (Press et al., 1992; Wang et al., 2006). Finally, a two-sample t test was performed on these z values to detect the between-group differences. In this study, however, we did not find significant connectivity differences ($P=0.13$) between the AD

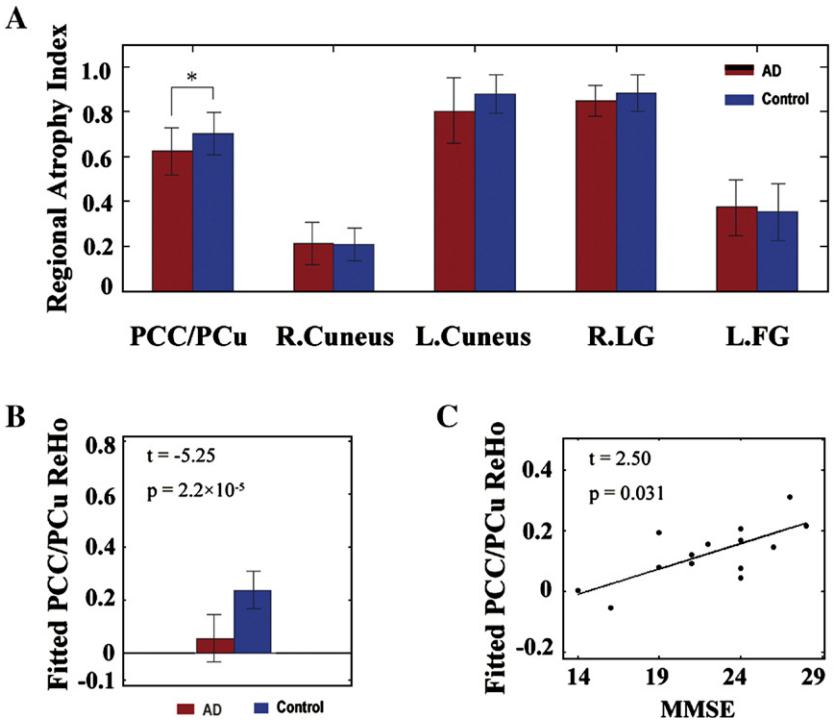

Fig. 4. (A) Mean regional atrophy index with standard error bars of each region in AD patients versus normal controls. Significantly more brain atrophy was observed in the AD patients in the PCC/PCu ($P=0.047$) but not in the right cuneus ($P=0.67$), left cuneus ($P=0.25$), right LG ($P=0.11$) and left FG ($P=0.25$). (B) Mean fitted ReHo of peak voxel with standard error (arbitrary units) bars in the PCC/PCu for each group after accounting for the regional atrophy (age and brain atrophy effects removed by regression). Between-group statistical significance is $P=2.1\times10^{-6}$ before (Fig. 2B) and $P=2.2\times10^{-5}$ after accounting for the effects of atrophy. (C) Scatter plot of fitted ReHo of peak voxel versus MMSE scores in the PCC/PCu in the AD patient group ($n=14$) after accounting for the regional atrophy (age and regional atrophy effects removed by regression). Each data point represents a single subject in the AD group. Statistical significance is $P=0.005$ before (Fig. 3B) and $P=0.031$ after accounting for the atrophy. The LFBF results in the PCC/PCu still remain significant with a moderate decrease in the statistical power after the atrophy was controlled. *$P<0.05$.

patients and normal controls. An explanation for the inconsistent results in the present study in comparison to the previous two studies could be that the PCC/PCu-hippocampus disconnectivity in the AD patients was associated with their subregions. Both of the previous studies involved the left hippocampus and BA 7/23/29/31 (Greicius et al., 2004) and a large anterior part of right hippocampus and BA 29 (Wang et al., 2006), while the present study mainly involved a small cluster in the right hippocampus (243 mm^3) and BA 31/7 (Fig. 2). Future investigations could be implemented to examine the changes of functional connections among the different subregions related to the PCC/PCu and hippocampus in AD patients.

Aside from the AD-related decreases aforementioned, increased coherences were also observed in the AD patients in the bilateral cuneus, right LG and left FG (Fig. 2, Table 2). However we did not find significant correlations between the coherence and the MMSE scores in the patient group. Functional neuroimaging studies of AD have indicated that these regions usually retain their functional capacity in the early stages of the disease (Grady et al., 1993; Mentis et al., 1996). Furthermore, we found that these regions are consistent with previous findings of increased functional activation in AD patients during the performance of cognitive tasks (Backman et al., 2000; Prvulovic et al., 2002). For example, Backman et al. (2000) reported that AD patients exhibited increased activation in the occipital cortex during priming. Prvulovic et al. (2002) found that the FG showed increased AD-related activation during visuospatial processing. These increased functional activations have been proposed as the involvement of compensatory mechanisms in AD (Backman et al., 2000; Prvulovic et al., 2002). Nevertheless, the compensatory role of these regions needs to be further described in the context of the resting state. Some investigators have suggested that memory is an important component of default activities during rest (Buckner et al., 2005; Greicius et al., 2003, 2004). Moreover, functional neuroimaging studies have indicated that the PCC/PCu may be involved in memory function, and decreased resting-state activity may reflect memory impairment in AD patients (Buckner et al., 2005; Greicius et al., 2004; Cabeza et al., 2002). Evidence from several studies has also suggested that the higher visual cortex and FG are involved in memory-related processing (Buckner and Wheeler, 2001; Kohler et al., 1998; Moscovitch et al., 1995). Combining these previous findings with our results, we suspect that AD-related LFBF reduction in the PCC/PCu might be compensated by the recruitment of the occipital lobe and the left FG.

It is important to note here that we took into account the impact of regional brain atrophy on the LFBF functional results (i.e. ReHo) shown in the PCC/PCu. Numerous studies have demonstrated that AD patients have more brain atrophy in the PCC/PCu than normal controls (Buckner et al., 2005; Baron et al., 2001; Chetelat et al., 2002). Brain atrophy may cause a partial volume effect in functional imaging techniques, especially in PET and SPECT that have low spatial resolution. The potential impact of

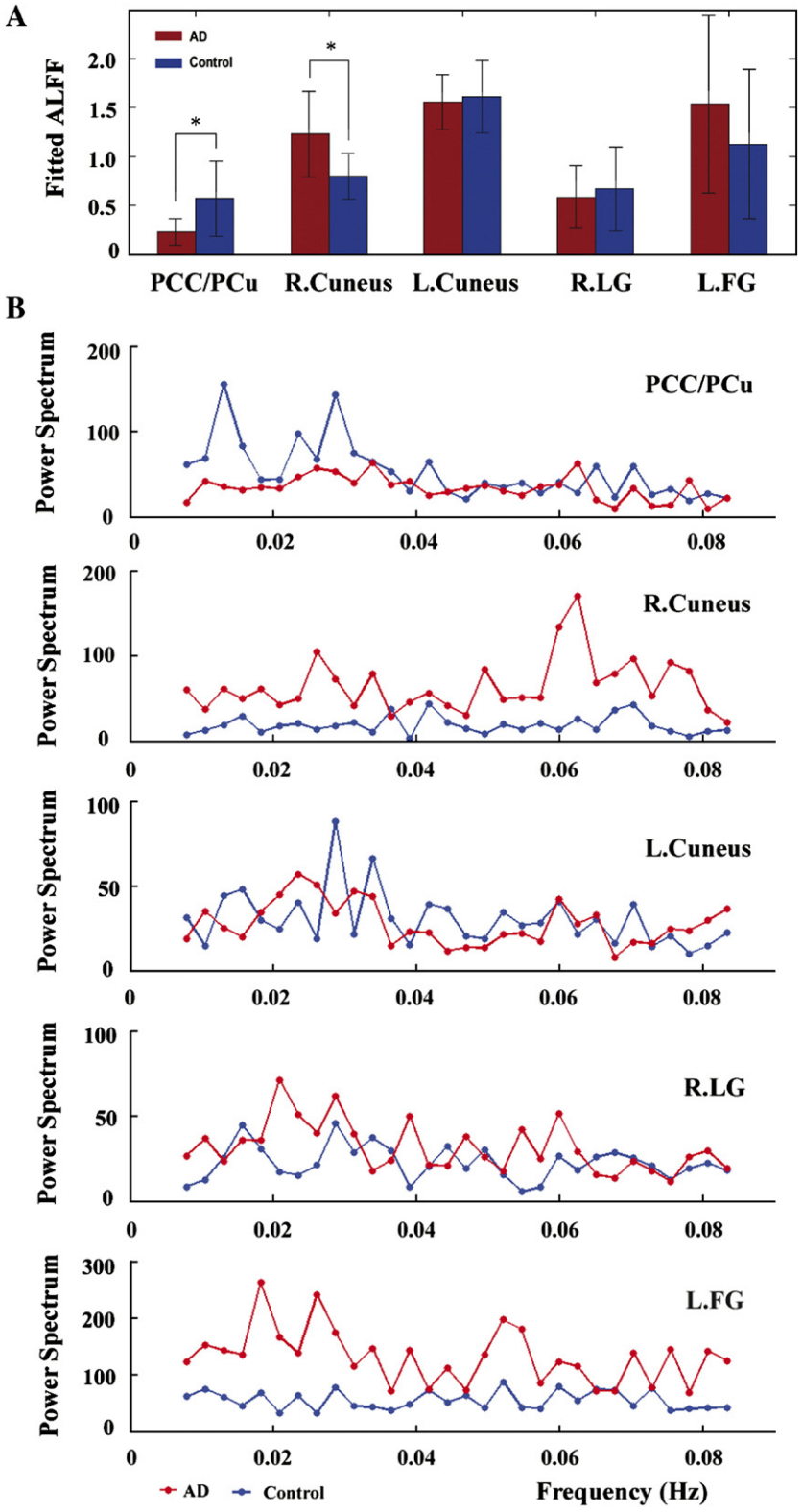

Fig. 5. (A) Mean fitted ALFF of peak voxel with standard error (arbitrary units) bars of each region in the AD patients versus normal controls (age effect removed by regression). The AD patients showed significant decreased ALFF in the PCC/PCu ($t=-3.04$, $P=0.005$) and increased ALFF in the right cuneus ($t=3.25$, $P=0.003$). There were no significant ALFF differences in the left cuneus ($t=-0.45$, $P=0.66$), right LG ($t=-0.56$, $P=0.58$) and left FG ($t=1.27$, $P=0.22$). *$P<0.05$. (B) Averaged Fourier power spectrums of each region in the AD patients (red lines) and normal controls (blue lines). The ALFF and power spectrums were calculated using the method proposed by Zang et al. (in press) (see Appendix 2 for details).

atrophy has been recognized in previous PET studies of AD using regional CMRglu (Bokde et al., 2001; Ibáñez et al., 1998). Several recent fMRI studies have also attempted to clarify the relationship between regional atrophy and BOLD signals during the performance of tasks (Johnson et al., 2000; Prvulovic et al., 2002; Remy et al., 2005). In this study, we found that AD patients showed significantly larger CSF volume in the PCC/PCu when compared with normal controls (Fig. 4A), suggesting the necessity for controlling the regional brain atrophy in the functional analysis. By taking into account the regional atrophy as a covariate, we found that statistical significance was reduced in both between-group differences in the PCC/PCu (Fig. 4B) and the correlation between the PCC/PCu ReHo and the MMSE scores (Fig. 4C). It implies that the AD-related LFBF results in the PCC/PCu can be at least partly explained by regional atrophy. With this in mind, we propose that the impact of regional brain atrophy on functional results should receive more attention in future functional imaging studies of neurodegenerative diseases.

In this study, we observed that the AD patients showed decreased regional coherence in the PCC/PCu both with and without accounting for regional brain atrophy. However, it is unclear whether such decreases simply imply a lower overall variance in the ambient BOLD activity (reflective of lower metabolic activity) or a reduced LFBF activity in the patients. To clarify this issue, we further measured the amplitude of low frequency fluctuations (ALFF) in this region using a power spectrum method proposed by Zang et al. (in press) (see Appendix 2 for details). It has been suggested that the ALFF may indicate regional spontaneous neuronal activity (Biswal et al., 1995; Zang et al., in press). Using this procedure, we found that the AD patients showed significantly decreased ALFF in the PCC/PCu ($P=0.005$, Fig. 5A). Moreover, the average Fourier power spectrum plot (Fig. 5B) also demonstrated that the changes in the power spectrum in the patients mainly focused on the lower frequency components (0.01–0.04 Hz). This power spectrum analysis indicates that our finding of the reduced PCC/PCu ReHo in the patients is a true reflection of the LFBF phenomenon. In addition, we also found that the right cuneus that showed AD-related ReHo increases in the present study had increased ALFF in the patients ($P=0.003$, Fig. 5A). There were no significant ALFF changes observed in the left cuneus, right LG and left FG (Fig. 5A).

Some methodological issues need to be addressed. First, we used the ReHo method (Zang et al., 2004) to detect the changes of regional LFBF coherence by quantifying the similarity of time series. The regional synchrony of fMRI time series can also be measured using the coefficients of spontaneous low frequency (COSLOF) index (Li et al., 2002). This index corresponds to the mean of the cross-correlation coefficients of LFBF between possible pairs of voxel time courses for a given brain region. For small regions, the COSLOF index and the ReHo reflect similar regional synchrony. In future AD studies, it would be interesting to compare the results of the two measurements. Secondly, in order to explore AD-related LFBF activity across the entire brain, the present study used a low sampling rate (TR=2 s) for the multi-slice acquisitions. Under such circumstance, the cardiac (usually larger than 1 Hz) and respiratory fluctuations cannot be completely removed according to the Nyquist sampling theorem (Lowe et al., 1998; Kiviniemi et al., 2005; Cordes et al., 2001). These aliasing physiological noises might reduce the specificity of the regional synchrony, or even further confound the observed ReHo differences between the two groups. In future, it would be helpful to estimate these effects by simultaneously recording the respiratory and cardiac cycle during the acquisition of whole-brain imaging data, or to remove these effects by focusing on some specific brain region with higher sampling rate (e.g. TR=500 ms). Thirdly, in this study, we used functional analysis results to guide the selection of ROIs and further calculate the regional atrophy index for each of them. It might be a limitation because brain atrophy is not isolated to specific gyri but a diffuse process in both aging and AD. However, the purpose of this study was to evaluate the impact of regional atrophy on regional LFBF analysis results. The implemented regional atrophy index, an operator-independent measurement, was used to address this specific issue. Though in the current study, the regional atrophy index was only employed to assess the effect of regional brain atrophy on the LFBF analysis. Further studies could be conducted to ascertain the relationship between regional brain atrophy (e.g. PCC/PCu or hippocampus) and the whole-brain LFBF activity. Finally, the present study only investigated the LFBF changes in AD patients. It is unclear whether the findings shown here are only specific to AD or might also be observed in other types of dementia such as vascular dementia and dementia with Lewy bodies. Further investigations on several different dementia groups might help to clarify this issue.

In summary, the AD patients exhibited changes of LFBF coherence in the PCC/PCu, the occipital and temporal lobes when compared with normal controls. These findings are compatible with previous functional imaging studies of early AD. Resting state fMRI, which has the advantages of no radiation exposure (compared to PET and SPECT) and easy application (compared to task-driven paradigms), has great potential for clinical diagnosis and treatment in the future. Our study also indicated that regional brain atrophy could be an important consideration in functional imaging studies of neurodegenerative diseases.

Acknowledgments

The authors would like to thank Dr. Chaozhe Zhu for providing his procedure concerning brain tissue segmentation and Mrs. Yuan Zhou for helpful comments. They would also like to thank Professor Keith Worsley of the Department of Mathematics and Statistics, McGill University and Mr. Zhang (John) Chen of the Montreal Neurological Institute, McGill University for their assistance in editing the manuscript. This work was partially supported by the Natural Science Foundation of China, Grant Nos. 30425004 and 60121302, State Commission of Science and Technology of China, Grant No. 2004CB318107.

Appendix A

In this study, regional coherence changes in AD patients were examined using the regional homogeneity (ReHo) method (Zang et al., 2004). The method is described as follows.

For a given voxel, we calculated Kendall's coefficient of concordance (KCC) (Kendall and Gibbons, 1990) of time series of this voxel with those of its nearest neighbors:

$$W = \frac{\Sigma(R_i)^2 - n(\bar{R})^2}{1/12k^2(n^3 - n)} \quad (1)$$

where W ranges from 0 to 1; $R_i = \Sigma_{j=1}^{k} r_{ij}$ where r_{ij} is the rank of the ith time point in the jth voxel; $\bar{R} = (n+1)k/2$ is the mean of

the R_i; n is the number of time points of each voxel time series (here $n=170$); and k is the number of time series within the measured cluster (here $k=27$, the central voxel plus its 26 neighbors). An individual W map (i.e. ReHo map) was obtained on a voxel by voxel basis for each subject resting-state data set.

Appendix B

Recent studies have suggested that the amplitude of low frequency fluctuations (ALFF) may be suggestive of regional spontaneous neuronal activity (Biswal et al., 1995; Zang et al., in press). In this study, we measured the ALFF differences between the AD patient group and normal control group using the method proposed by Zang et al. (in press). Briefly, the filtered time series obtained from data preprocessing (see Materials and methods) was first transformed into the frequency domain using a fast Fourier transform (FFT) and the power spectrum was then obtained. Since the power at a given frequency is proportional to the square of the amplitude of this frequency component in the original time series in the time domain, we calculated the square root of the power spectrum at each frequency and averaged these across 0.01–0.08 Hz at each voxel. This resulting ALFF value was further standardized by dividing by the global mean value. Finally, a two-tailed two-sample t test was performed on the ALFF of each region to compare the difference between the AD patient and normal controls. Age was taken as a confounding covariate in this analysis. Statistical differences in the ALFF of each region are shown in Fig. 5A and the average Fourier power spectrums are shown in Fig. 5B.

References

American Psychiatric Association, 1994. DSM-IV: Diagnostic and Statistical Manual of Mental Disorders, 4th ed. Am. Psychiatric Assoc. Press, Washington, DC.

Anand, A., Li, Y., Wang, Y., Wu, J., Gao, S., Bukhari, L., et al., 2005. Activity and connectivity of brain mood regulating circuit in depression: a functional magnetic resonance study. Biol. Psychiatry 57, 1079–1088.

Arieli, A., Sterkin, A., Grinvald, A., Aertsen, A., 1996. Dynamics of ongoing activity: explanation of the large variability in evoked cortical responses. Science 273, 1868–1871.

Backman, L., Almkvist, O., Nyberg, L., Andersson, J., 2000. Functional changes in brain activity during priming in Alzheimer's disease. J. Cogn. Neurosci. 12, 134–141.

Baron, J.C., Chételat, G., Desgranges, B., Perchey, G., Landeau, B., de la Sayette, V., et al., 2001. In vivo mapping of gray matter loss with voxel-based morphometry in mild Alzheimer's disease. NeuroImage 14, 298–309.

Biswal, B., Yetkin, F.Z., Haughton, V.M., Hyde, J.S., 1995. Functional connectivity in the motor cortex of resting human brain using echo-planar MRI. Magn. Reson. Med. 34, 537–541.

Biswal, B.B., Van Kylen, J., Hyde, J.S., 1997. Simultaneous assessment of flow and BOLD signals in resting-state functional connectivity maps. NMR Biomed. 10, 165–170.

Bokde, A.L., Pietrini, P., Ibáñez, V., Furey, M.L., Alexander, G.E., Graff-Radford, N.R., et al., 2001. The effect of brain atrophy on cerebral hypometabolism in the visual variant of Alzheimer disease. Arch. Neurol. 58, 480–486.

Buckner, R.L., Wheeler, M.E., 2001. The cognitive neuroscience of remembering. Nat. Rev., Neurosci. 2, 624–634.

Buckner, R.L., Snyder, A.Z., Sanders, A.L., Raichle, M.E., Morris, J.C., 2000. Functional brain imaging of young, nondemented, and demented older adults. J. Cogn. Neurosci. 12, 24–34.

Buckner, R.L., Snyder, A.Z., Shannon, B.J., LaRossa, G., Sachs, R., Fotenos, A.F., et al., 2005. Molecular, structural, and functional characterization of Alzheimer's disease: evidence for a relationship between default activity, amyloid, and memory. J. Neurosci. 25, 7709–7717.

Cabeza, R., Dolcos, F., Graham, R., Nyberg, L., 2002. Similarities and differences in the neural correlates of episodic memory retrieval and working memory. NeuroImage 16, 317–330.

Cao, Q.J., Zang, Y.F., Sun, L., Sui, M.Q., Long, X.Y., Zou, Q.H., Wang, Y. F., 2006. Abnormal neural activity in children with attention deficit hyperactivity disorder: a resting-state functional magnetic resonance imaging study. NeuroReport 17, 1033–1036.

Chawluk, J.B., Dann, R., Alavi, A., Hurtig, H.I., Gur, R.E., Resnick, S., et al., 1990. The effect of focal cerebral atrophy in positron emission tomographic studies of aging and dementia. Radiation 17, 797–804.

Chetelat, G., Desgranges, B., De La Sayette, V., Viader, F., Eustache, F., Baron, J.C., 2002. Mapping gray matter loss with voxel-based morphometry in mild cognitive impairment. NeuroReport 13, 1939–1943.

Cordes, D., Haughton, V., Arfanakis, K., Carew, J.D., Turski, P.A., Moritz, C.H., et al., 2001. Frequencies contributing to functional connectivity in the cerebral cortex in "resting-state" data. Am. J. Neuroradiol. 22, 1326–1333.

Cox, R.W., 1996. AFNI software for analysis and visualization of functional magnetic resonance neuroimages. Comput. Biomed. Res. 29, 162–173.

Cox, R.W., Jesmanowicz, A., 1999. Real-time 3D image registration for functional MRI. Magn. Reson. Med. 42, 1014–1018.

Fox, M.D., Snyder, A.Z., Vincent, J.L., Corbetta, M., Van Essen, D.C., Raichle, M.E., 2005. The human brain is intrinsically organized into dynamic, anticorrelated functional networks. Proc. Natl. Acad. Sci. U. S. A. 102, 9673–9678.

Grady, C.L., Haxby, J.V., Horwitz, B., Gillette, J., Salerno, J.A., Gonzalez-Aviles, A., 1993. Activation of cerebral blood flow during a visuoperceptual task in patients with Alzheimer-type dementia. Neurobiol. Aging 14, 35–44.

Greicius, M.D., Krasnow, B., Reiss, A.L., Menon, V., 2003. Functional connectivity in the resting brain: a network analysis of the default mode hypothesis. Proc. Natl. Acad. Sci. U. S. A. 100, 253–258.

Greicius, M.D., Srivastava, G., Reiss, A.L., Menon, V., 2004. Default-mode network activity distinguishes Alzheimer's disease from healthy aging: evidence from functional MRI. Proc. Natl. Acad. Sci. U. S. A. 101, 4637–4642.

Hampson, M., Peterson, B.S., Skudlarski, P., Gatenby, J.C., Gore, J.C., 2002. Detection of functional connectivity using temporal correlations in MR images. Hum. Brain Mapp. 15, 247–262.

He, Y., Zang, Y.F., Jiang, T.Z., Liang, M., Gong, G.L., 2004. Detecting functional connectivity of the cerebellum using low frequency fluctuations (LFFs). In: Barillot, C., Haynor, D.R., Hellier, P. (Eds.), Lect Notes Comput Sci, vol. 3217. Springer-Verlag, Berlin, pp. 907–915.

He, Y., Zang, Y.F., Jiang, T.Z., Gong, G.L., Xie, S., Xiao, J.X., 2006. Handedness-related functional connectivity using low-frequency blood oxygenation level-dependent fluctuations. NeuroReport 17, 5–8.

Herholz, K., Salmon, E., Perani, D., Baron, J.C., Holthoff, V., Frolich, L., et al., 2002. Discrimination between Alzheimer dementia and controls by automated analysis of multicenter FDG PET. NeuroImage 17, 302–316.

Holmes, A.P., Friston, K.J., 1998. Generalisability, random effects and population inference. NeuroImage 7, S754.

Ibáñez, V., Pietrini, P., Alexander, G.E., Furey, M.L., Teichberg, D., Rajapakse, J.C., 1998. Regional glucose metabolic abnormalities are not the result of atrophy in Alzheimer's disease. Neurology 50, 1585–1593.

Jiang, T.Z., He, Y., Zang, Y.F., Weng, X.C., 2004. Modulation of functional connectivity during the resting state and the motor task. Hum. Brain Mapp. 22, 63–71.

Johnson, S.C., Saykin, A.J., Baxter, L.C., Flashman, L.A., Santulli, R.B., McAllister, T.W., et al., 2000. The relationship between fMRI activation and cerebral atrophy: comparison of normal aging and Alzheimer disease. NeuroImage 11, 179–187.

Karas, G.B., Burton, E.J., Rombouts, S.A., Van Schijndel, R.A., O'Brien, J.T., Scheltens, P., et al., 2003. A comprehensive study of gray matter loss in patients with Alzheimer's disease using optimized voxel-based morphometry. NeuroImage 18, 895–907.

Kendall, M., Gibbons, J.D.R., 1990. Correlation Methods. Oxford Univ. Press, Oxford.

Kiviniemi, V., Kantola, J.H., Jauhiainen, J., Tervonen, O., 2004. Comparison of methods for detecting nondeterministic BOLD fluctuation in fMRI. Magn. Reson. Imaging 22, 197–203.

Kiviniemi, V., Ruohonen, J., Tervonen, O., 2005. Separation of physiological very low frequency fluctuation from aliasing by switched sampling interval fMRI scans. Magn. Reson. Imaging 23, 41–46.

Kohler, S., McIntosh, A.R., Moscovitch, M., Winocur, G., 1998. Functional interactions between the medial temporal lobes and posterior neocortex related to episodic memory retrieval. Cereb. Cortex 8, 451–461.

Leon, M.J., Convit, A., Wolf, O.T., Tarshish, C.Y., DeSanti, S., Rusinek, H., 2001. Prediction of cognitive decline in normal elderly subjects with 2-[18F] fluoro-2-deoxy-D-glucose/positron-emission tomography (FDG/PET). Proc. Natl. Acad. Sci. U. S. A. 98, 10966–10971.

Leopold, D.A., Murayama, Y., Logothetis, N.K., 2003. Very slow activity fluctuations in monkey visual cortex: implications for functional brain imaging. Cereb. Cortex 13, 422–433.

Li, S.J., Li, Z., Wu, G., Zhang, M.J., Franczak, M., Antuono, P.G., 2002. Alzheimer disease: evaluation of a functional MRI index as a marker. Radiology 225, 253–259.

Liu, H., Liu, Z., Liang, M., Hao, Y., Tan, L., Kuang, F., Yi, Y., Xu, L., Jiang, T., 2006. Decreased Regional Homogeneity in Schizophrenia: a Resting State fMRI study. NeuroReport 17, 19–22.

Lowe, M.J., Mock, B.J., Sorenson, J.A., 1998. Functional connectivity in single and multislice echoplanar imaging using resting state fluctuations. NeuroImage 7, 119–132.

Lowe, M.J., Phillips, M.D., Lurito, J.T., Mattson, D., Dzemidzic, M., Mathews, V.P., 2002. Multiple sclerosis: low-frequency temporal blood oxygen level-dependent fluctuations indicate reduced functional connectivity—initial results. Radiology 224, 184–192.

Lustig, C., Snyder, A.Z., Bhakta, M., O'Brien, K.C., McAvoy, M., Raichle, M.E., et al., 2003. Functional deactivations: change with age and dementia of the Alzheimer type. Proc. Natl. Acad. Sci. U. S. A. 100, 14504–14509.

Maldjian, J.A., 2001. Functional connectivity MR imaging: fact or artifact? [comment]. Am. J. Neuroradiol. 22, 239–240.

Maxim, V., Xendur, L., Fadili, J., Suckling, J., Gould, R., Howard, R., 2005. Fractional Gaussian noise, functional MRI and Alzheimer's disease. NeuroImage 25, 141–158.

McKhann, G., Drachman, D., Folstein, M., Katzman, R., Price, D., Stadlan, M., 1984. Clinical diagnosis of Alzheimer's disease: report of the NINCDS-ADRDA Work Group under the auspices of the Department of Health and Human Services Task Force on Alzheimer's Disease. Neurology 34, 39–44.

Mentis, M.J., Horwitz, B., Grady, C.L., Alexander, G.E., VanMeter, J.W., Maisog, J.M., 1996. Visual cortical dysfunction in Alzheimer's disease evaluated with a temporally graded "stress test" during PET. Am. J. Psychiatry 153, 32–40.

Morris, J.C., 1993. Clinical dementia rating. Neurology 43, 2412–2414.

Moscovitch, C., Kapur, S., Kohler, S., Houle, S., 1995. Distinct neural correlates of visual long-term memory for spatial location and object identity: a positron emission tomography study in humans. Proc. Natl. Acad. Sci. U. S. A. 92, 3721–3725.

Nestor, P.J., Scheltens, P., Hodges, J.R., 2004. Adance in the early detection of Alzheimer's disease. Nat. Rev., Neurosci. 5, 34–41.

Poline, J.B., Worsley, K.J., Evans, A.C., Friston, K.J., 1997. Combining spatial extent and peak intensity to test for activations in functional imaging. NeuroImage 5, 83–96.

Press, W.H., Teukolsky, S.A., Vetterling, W.T., Flannery, B.P., 1992. Numerical Recipes in C, 2nd ed. R. U. K. Cambridge Univ. Press, Cambridge.

Prvulovic, D., Hubl, D., Sack, A.T., Melillo, L., Maurer, K., Frflich, L., 2002. Functional imaging of visuospatial processing in Alzheimer's disease. NeuroImage 17, 1403–1414.

Raichle, M.E., MacLeod, A.M., Snyder, A.Z., Powers, W.J., Gusnard, D.A., Shulman, G.L., 2001. A default mode of brain function. Proc. Natl. Acad. Sci. U. S. A. 16, 676–682.

Reiman, E.M., Caselli, R.J., Yun, L.S., Chen, K., Bandy, D., Minoshima, S., et al., 1996. Preclinical evidence of Alzheimer's disease in persons homozygous for the e4 allele for Apolipoprotein E. N. Engl. J. Med. 334, 752–758.

Remy, F., Mirrashed, F., Campbell, B., Richter, W., 2005. Verbal episodic memory impairment in Alzheimer's disease: a combined structural and functional MRI study. NeuroImage 25, 253–266.

Rombouts, S.A., Barkhof, F., Witter, M.P., Scheltens, P., 2000. Unbiased whole-brain analysis of gray matter loss in Alzheimer's disease. Neurosci. Lett. 19, 231–233.

Rombouts, S.A., Stam, C.J., Kuijer, J.P., Scheltens, P., Barkhof, F., 2003. Identifying confounds to increase specificity during a "no task condition". Evidence for hippocampal connectivity using fMRI. NeuroImage 20, 1236–1245.

Rombouts, S.A., Barkhof, F., Goekoop, R., Stam, C.J., Scheltens, P., 2005. Altered resting state networks in mild cognitive impairment and mild Alzheimer's disease: an fMRI study. Hum. Brain Mapp. 26, 231–239.

Salvador, R., Suckling, J., Coleman, M.R., Pickard, J.D., Menon, D., Bullmore, E.D., 2005. Neurophysiological architecture of functional magnetic resonance images of human brain. Cereb. Cortex 15, 1332–1342.

Salmon, E., Collette, F., Degueldre, C., Lemaire, C., Franck, G., 2000. Voxel-based analysis of confounding effects of age and dementia severity on cerebral metabolism in Alzheimer's disease. Hum. Brain Mapp. 10, 39–48.

Small, G.W., Ercoli, L.M., Silverman, D.H., Huang, S.C., Komo, S., Bookheimer, S.Y., et al., 2000. Cerebral metabolic and cognitive decline in persons at genetic risk for Alzheimer's disease. Proc. Natl. Acad. Sci. U. S. A. 97, 6037–6042.

Steriade, M., McCormick, D.A., Sejnowski, T.J., 1993. Thalamocortical oscillations in the sleeping and aroused brain. Science 262, 679–685.

Tanna, N.K., Kohn, M.I., Horwich, D.N., Jolles, P.R., Zimmerman, R.A., Alves, W.M., et al., 1991. Analysis of brain and cerebrospinal fluid volumes with MR imaging: Impact on PET data correction for atrophy. Part II. Aging and Alzheimer dementia. Radiology 178, 123–130.

Talairach, J., Tournoux, P.A., 1998. Coplanar Stereotactic Atlas of the Human Brain. Thieme, Stuttgart.

Volkow, N.D., Zhu, W., Felder, C.A., Mueller, K., Welsh, T.F., Wang, G.J., 2002. Changes in brain functional homogeneity in subjects with Alzheimer's disease. Psychiatry Res. 15, 39–50.

Wang, L., Zang, Y.F., He, Y., Zhang, X.Q., Jiang, T.Z., Liang, M., Tian, L.X., Wu, T., Li, K.C., 2006. Changes of hippocampal connectivity in the early stages of Alzheimer's disease: evidence from resting state fMRI. NeuroImage 31, 496–504.

Zang, Y.F., Jiang, T.Z., Lu, Y.L., He, Y., Tian, L.X., 2004. Regional homogeneity approach to fMRI data analysis. NeuroImage 22, 394–400.

Zang, Y.F., He, Y., Zhu, C.Z., Cao, Q.J., Sui, M.Q., Liang, M., Tian, L. X., Jiang, T.Z., Wang, Y.F., in press. Altered baseline brain activity in children with ADHD revealed by resting-state functional MRI. Brain Dev.

Zhu, C.Z., Jiang, T.Z., 2003. Multi-context fuzzy clustering for separation of brain tissues in MR images. NeuroImage 18, 685–696.